Check for updates

ARTICLE

Cathepsin B modulates microglial migration and phagocytosis of amyloid β in Alzheimer's disease through PI3K-Akt signaling

Muzhou Jiang[1,2], Dan Zhao[3], Yue Zhou[4], Wei Kong[2], Zhen Xie[2], Yijie Xiong[5], Yanhui Li[5], Shuxuan Zhao[2], Xueshuai Kou[2], Simeng Zhang[2], Rui Meng[2], Yaping Pan[1], Zhou Wu[6], Hiroshi Nakanishi[7], Juan Zhao[8], Hui Li[2,9], Zhenzhen Quan [2], Li Lin[1 ✉], Hong Qing [2,9] and Junjun Ni [2 ✉]

The approval of anti-amyloid β (Aβ) monoclonal antibodies (lecanemab) for the treatment of patients with early preclinical stage of Alzheimer's disease (AD) by the Food and Drug Administration, suggests the reliability and importance of brain Aβ clearance for AD therapy. Microglia are the main phagocytes that clear Aβ in the brain, but the underlying regulatory mechanism is unclear. Here, we investigate the critical role of cathepsin B (CatB) in modulating microglial Aβ clearance from mouse brain. Wild-type or $CatB^{-/-}$ mice were injected with Aβ into the hippocampus from 1 to 3 weeks. Mice were evaluated for cognitive change, Aβ metabolism, neuroinflammation. Microglia and neuron cultures were prepared to verify the in vivo results. The statistical analyses were performed by student's t test, one-way ANOVA with a post hoc Tukey's test using the GraphPad Prism software package. CatB deficiency significantly reduces Aβ clearance efficiency and aggravates mouse cognitive decline. Exogenous Aβ markedly increases CatB expression in activated microglia. Transcriptome analysis and in vitro cell culture experiments demonstrate that CatB is associated with gene clusters involved in migration, phagocytosis, and inflammation. In addition, transcriptome analysis and immunoblotting suggest that CatB modulates microglial Aβ clearance via PI3K-AKT activation. Our study unveils a previously unknown role of CatB in promoting microglial functionality during Aβ clearance.

Neuropsychopharmacology; https://doi.org/10.1038/s41386-024-01994-0

INTRODUCTION

Abnormal β-amyloid is a key pathological hallmark of Alzheimer's disease (AD), according to the 2018 National Institute on Aging and the Alzheimer's Association Research Framework, and a major target in AD research and drug development [1]. Cholinesterase inhibitors and the N-methyl-D-aspartate receptor antagonist, memantine, have been approved by the United States Food and Drug Administration (FDA) as symptomatic treatments for patients with moderate-to-severe AD; however, no disease-modifying or preventive treatments were available for AD until Leqembi (lecanemab) was approved for treatment of early stage AD by the FDA [2]. Lecanemab is a humanized IgG1 monoclonal antibody that binds to Aβ soluble protofibrils with high affinity [2], and the selective binding of lecanemab to soluble Aβ facilitates microglial Aβ clearance. However, the mechanisms by which microglia clear Aβ has not been fully elucidated.

Microglia are the primary immune cells of the central nervous system, with functions comparable to those of blood macrophages, including phagocytic and inflammatory properties [3]. Microglia constantly survey the surrounding environment for any changes or the presence of pathogens by extending and retracting their processes [4]. Comprehensive single-cell RNA sequencing analysis of samples from AD, amyotrophic lateral sclerosis, and aging have identified a rare subset of microglia, disease-associated microglia (DAM), that is conserved between mice and humans [5]. There is accumulating evidence that DAM responses arise as a protective mechanism that functions to contain and remove neuronal damage [6].

Cathepsin B (CatB, EC 3.4.22.1), originally named CatB1, was the first, and remains the best-characterized, member of the C1 family of papain-like, lysosomal cysteine peptidases. First purified to homogeneity from the human liver in 1973 [7], CatB is ubiquitously expressed in most cell and tissue types [8]. Further, CatB is involved in AD pathology in microglia or neurons, either through microglia-mediated neuroinflammation or abnormal neuronal digestion systems [9–11]; however, the communication between microglia and neurons, along with CatB expression in both cell types, makes it difficult to determine the exact relationship between CatB and Aβ.

To eliminate the effects of CatB in Aβ production by neurons, we stereotaxically injected Aβ into the hippocampus of wild-type (WT) and $CatB^{-/-}$ mice, to allow examination of the role of CatB in

[1]Department of Periodontics, Liaoning Provincial Key Laboratory of Oral Diseases, School and Hospital of Stomatology, China Medical University, Shenyang, China. [2]Key Laboratory of Molecular Medicine and Biotherapy, School of Life Science, Beijing Institute of Technology, Beijing, China. [3]Department of Implant Dentistry, Beijing Stomatological Hospital, Capital Medical University, Beijing, China. [4]Department of Hematology, the Affiliated Suzhou Hospital of Nanjing Medical University, Suzhou Municipal Hospital, Suzhou, China. [5]Beijing 171 Middle School, Beijing, China. [6]Department of Aging Science and Pharmacology, OBT Research Center, Faculty of Dental Science, Kyushu University, Fukuoka, Japan. [7]Department of Pharmacology, Faculty of Pharmacy, Yasuda Women's University, Hiroshima, Japan. [8]Aerospace Medical Center, Aerospace Center Hospital, Beijing, China. [9]Department of Biology, Shenzhen MSU-BIT University, Shenzhen, China. ✉email: linli@cmu.edu.cn; nijunjun@bit.edu.cn

Aβ clearance. Remarkably, $CatB^{-/-}$ mice exhibited relatively weak Aβ clearance efficiency and aggravated cognitive deficits relative to WT mice after Aβ administration. Our results suggest that microglial CatB is involved in microglial migration, acute neuroinflammation, and phagocytosis dependent on the PI3K-AKT pathway.

MATERIALS AND METHODS
Animals
WT and CatB knock-out of C57BL/6 background were kept and bred in the Animal room of Beijing Institute of Technology and China Medical University. The $CatB^{-/-}$ mice were obtained by crossing male and female $CatB^{+/-}$ mice [3]. The lack of gene expression was confirmed by examining genomic DNA isolated from tail biopsies using a CatB-exon 4-specific
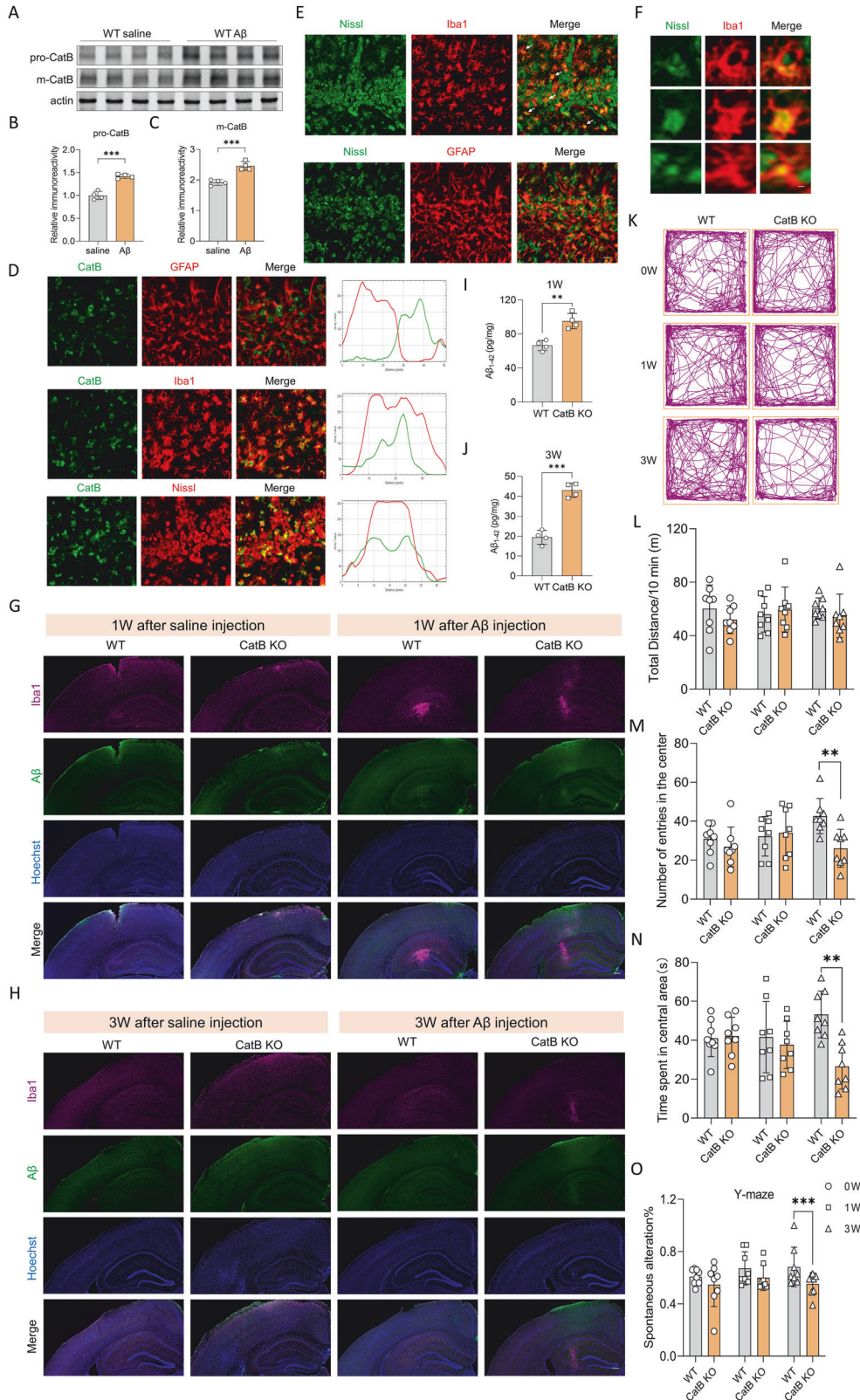
Fig. 1 CatB deficiency attenuated Aβ clearance in the mouse hippocampus. A Immunoblots of CatB in the hippocampus of WT mice after administration of Aβ or saline for 1 week. Quantitative analysis of pro-CatB (**B**) and m-CatB (**C**) shown in (**A**). Columns and bars represent mean ± SD ($n = 4$ mice). Asterisks indicate significant differences compared with the saline group (***$p < 0.001$, Student's t test). **D** Confocal laser scanning microscope (CLSM) images of GFAP (red), Iba1 (red), or Nissl (red) with CatB (green) in the hippocampus of WT mice after administration of Aβ for 1 week. Scale bar, 10 μm. The right profile plots fluorescence intensity (values from 0 to 250) of CatB (green) with GFAP (red), Iba1 (red), or Nissl (red) at the position along the white lines in the corresponding left panels, respectively. **E** CLSM images of neurons (Nissl, green) with microglia (Iba1, red) or astrocytes (GFAP, red) in the hippocampus of WT mice after administration of Aβ for 1 week. Scale bar, 10 μm. **F** Close-up of the images shown in (**E**) representing different stages of microglial phagocytosis of neurons. Scale bar, 5 μm. **G**, **H** Confocal laser scanning microscope images of Iba1 (magenta), Aβ (green), and Hoechst (blue) in the hippocampus of wild-type (WT) and CatB$^{-/-}$ mice after administration of Aβ or saline for 1 week (**A**) or 3 weeks (**B**). Scale bar, 100 μm. The amount of residual Aβ in the hippocampus of WT and CatB$^{-/-}$ mice after administration of Aβ for 1 week (**I**) and 3 weeks (**J**). Columns and bars represent mean ± SD ($n = 4$ mice). Asterisks indicate significant differences compared with WT mice (**$p < 0.01$, ***$p < 0.001$, Student's t test). **K** Representative track plots of WT and CatB$^{-/-}$ mice after administration of Aβ in the open-field test. Quantification of the total distance (**L**), average number of entries (**M**), and time spent (**N**) in the central area in the open-field test ($n = 8$ mice/group). Error bars represent mean ± SD. Asterisks indicate a significant difference from the indicated value (*$p < 0.05$, **$p < 0.01$, one-way ANOVA). **O** Average alteration in the number of entries of WT mice and CatB$^{-/-}$ mice after administration of Aβ in the Y-maze test ($n = 8$ mice/group). Error bars represent mean ± SD. Asterisks indicate a significant difference from the indicated value (***$p < 0.001$, **$p < 0.01$, one-way ANOVA).

polymerase chain reaction (PCR) with MCB11 primers (5′-GGTTGCGTTCGG TGAGG-3′) and MCBGT (5′-AACAAGAGCCGCAGGAGC-3′). Four-month-old WT and CatB$^{-/-}$ mice were divided into two groups. Both groups were fed with PLX-3397 (MedCheme Express, HY-16749), the CSF1R inhibitor, for 21 days to delete the microglia in the brain. After microglia elimination, 1 μg OAβ was infused into the brain of mice in both groups. Matched number of mice in both genders were used in the study. All animal studies were carried out following the guidelines contained in the Regulation of Laboratory Animals (Beijing Institute of Technology and China Medical University) and under the protocols approved by the Institutional Animal Care and Use Committee review panels at Beijing Institute of Technology.

Generation of CatB knockdown cells

A microglial CatB knockdown cell line (MG7) was established by using immortalized mouse microglial cell line, MG6 cells, and a commercially available clustered regularly interspaced short palindromic repeats (CRISPR) and homology-directed repair (HDR) (ORIGENE, Cat#KN303984) on MG6 cells via CRISPR and HDR. Positive cells were selected with 2 μg/ml puromycin (InvivoGen, Cat#ant-pr) for 15 days. A single-cell clone was picked up and continued to culture. CatB expression was assessed by Q-PCR and immunoblotting. During the generation, we also included scramble control gRNA (SKU GE100003, ORIGENE, Cat#KN303984) to serve as a negative control. Positive clones were collected and cultured. However, some positive cell gene KO may occur in one allele (heterozygous).

Cell viability assay

MG6 cells were seeded in 96-well plates overnight (5×10^3 cells/well) and then cultured by treatment with different concentrations ranging from 0 to 10 μM of PI3K inhibitor LY294002 (Sigma; L9908). A cell viability assay was performed using a Cell-Counting Kit (CCK-8) (Dojindo, Kumamoto, Japan) according to the previously described methods [12]. The optical density was read at a wavelength of 450 nm with a microplate reader. The cell viability was calculated by dividing the optical density of LY294002-treated group by that of nontreated group. LY294002 up to 2 μM had no significant toxic effect on MG6 cells, therefore 2 μM LY294002 was used in further experiments.

Cell culture

The mouse microglial cell line MG6 (RCB2403, Riken BioResource Center) was maintained in DMEM containing 10% fetal bovine serum (Gibco) supplemented with 2 mg/ml Glucose (Gibco), Penicillin-Streptomycin (Gibco), 10 μg/ml insulin and 100 M β-mercaptoethanol. The maximum number of passages for cell lines was 20. Primary microglia were prepared from the neonatal cortex following the previously described methods [13]. The cultured MG6 cells were stimulated with Aβ for 0, 5, 15, 30, 60, and 120 min. MG6 cells were treated with LY294002 (Sigma; L9908) for 30 min following Aβ stimulation. There were three independent dissections in total.

Stereotactic injection of Aβ

Four-month-old WT and CatB$^{-/-}$ mice were anesthetized to full muscle relaxation with ketamine and xylazine (100 mg/kg and 10 mg/kg,

respectively), and placed in a stereotaxic device. Surgeries were conducted on heated plates, and body temperature was monitored throughout the procedure. The skull was exposed and a hole was drilled into the skull for injection (bregma −2.0 mm, −1.8 mm lateral to midline, 2 mm below the dura). Human synthetic monomeric Aβ$_{1-42}$ (Nanjing Peptide Biotech Ltd) was incubated at 37 °C for 3 days to prepare the Aβ oligomers. A microsyringe (25 G) was used to infuse 1 μg OAβ into the brain over 2 min and was left in place for an additional 3 min and withdrawn slowly [14]. The incision was closed, and the mice were maintained at 37 °C until fully recovered from anesthesia. 0.2 mg/kg buprenorphine was used immediately after surgery to reduce pain.

Real-time quantitative PCR analysis

Total RNA from tissue and cells was extracted using RNAiso Plus (Takara, Hoto-ku, Osaka, Japan) according to the manufacturer's instructions. A total of 1 μg RNA was reverse transcribed to cDNA using the QuantiTect Reverse Transcription Kit (Qiagen, Japan). After an initial denaturation step at 95 °C for 5 min, temperature cycling was initiated. Each cycle consisted of denaturation at 95 °C for 5 s, annealing at 60 °C for 10 s, and elongation for 30 s. In total, 40 cycles were performed. The cDNA was amplified in duplicate using a Rotor-Gene SYBR Green RT-PCR Kit (Qiagen, Japan) with a Corbett Rotor-Gene RG-3000A Real-Time PCR System. The data were evaluated using the RG-3000A software program (version Rotor-Gene 6.1.93, Corbett). The primers used were listed in Table S1. For normalization, an endogenous control (actin) was assessed to control for the cDNA input, and the relative units were calculated by a comparative Ct method. Experiments were repeated three times, and the results are presented as the means of the ratios ± SEM.

Statistical analysis

All data are representative of at least three different experiments. Data are means ± SEM of three independent experiments. The statistical analyses were performed by student's t test, one-way ANOVA with a post hoc Tukey's test using the GraphPad Prism software package (GraphPad Software). A value of $p < 0.05$ was considered to indicate statistical significance.

RESULTS
CatB deficiency weakened Aβ clearance ability and induced memory decline in mice

Microglia can promote neuronal Aβ production by triggering neuroinflammation. Conversely, they can also contribute to extracellular Aβ clearance, making it difficult to determine whether microglia are beneficial or detrimental in the context of Aβ [15]. We administered Aβ into the hippocampus of mice to examine the direct effects of microglia on exogenous Aβ. Lysosomal proteases can contribute to AD by proteolytic processing or via autophagy-mediated clearance of accumulated material, including Aβ [16]. CatB is a typical cysteine lysosomal protease involved in AD pathological processes. In this study, 1 week after Aβ injection, levels of both pro- and mature-type

Figure 1
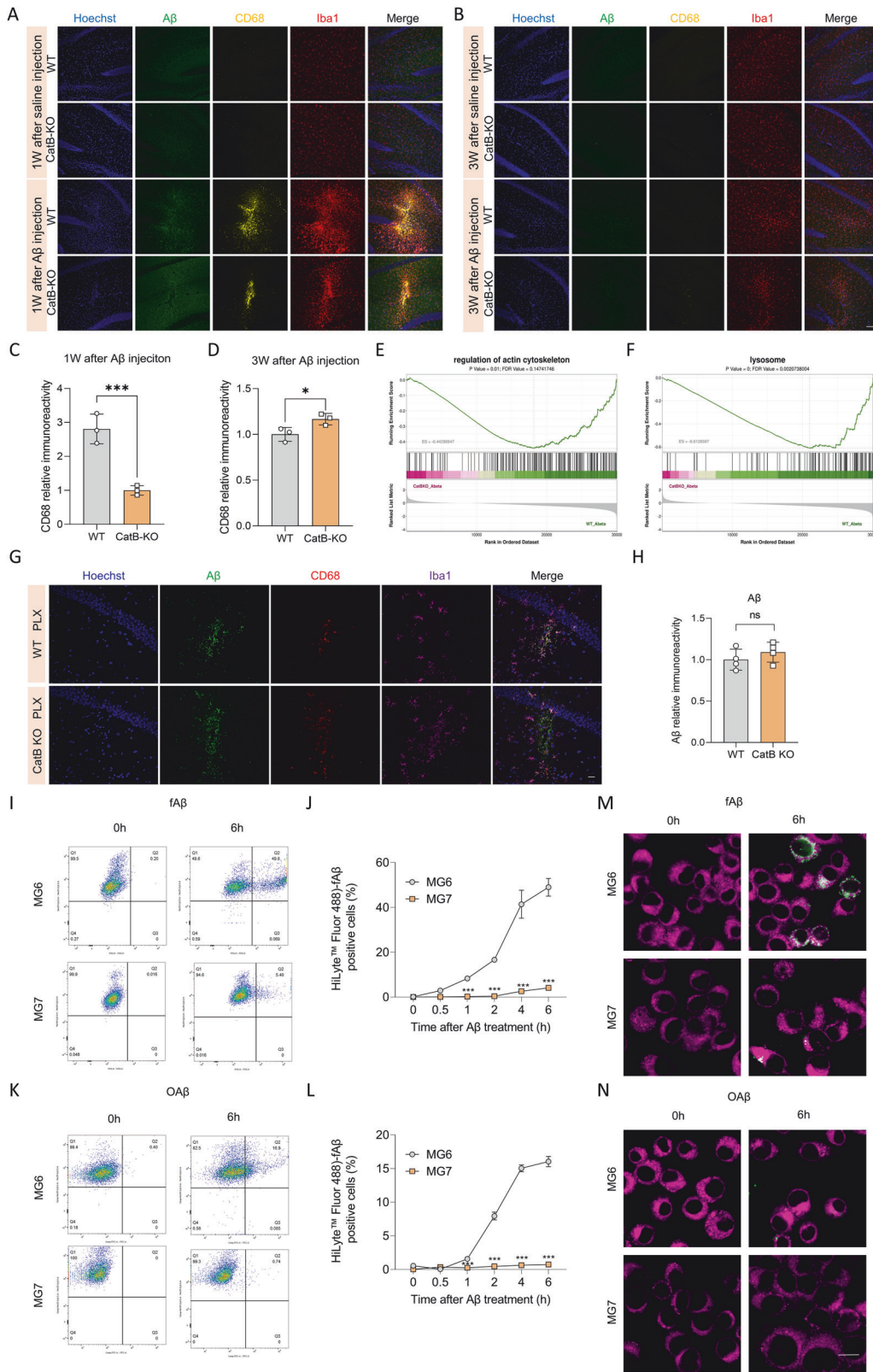
CatB were increased in the hippocampus of WT mice (Fig. 1A–C). CatB is expressed in both neurons and microglia in the mouse brain [17]. To examine the location of CatB in the brain after Aβ injection, we co-stained CatB with microglia (Iba1), astrocytes (GFAP), and neurons (NISSL) in WT mice after Aβ administration for 1 week. Clear CatB immune signals were detected in both microglia and neurons, but not in astrocytes (Fig. 1D). Therefore, we hypothesized that Aβ may increase CatB in microglia and neurons, or that microglia potentially phagocytes damaged neurons after Aβ injection. To test this hypothesis, we co-stained

Fig. 2 CatB deficiency attenuates microglial phagocytosis activity of Aβ. Confocal laser scanning microscope (CLSM) images of Aβ (green), CD68 (dark red), and Iba1 (red) with Hoechst (blue) in the injected area of wild-type (WT) and $CatB^{-/-}$ mouse hippocampus after Aβ or saline administration for 1 week (**A**) or 3 weeks (**B**). Scale bar, 50 μm. **C, D** Relative fluorescent density of CD68 in the images shown in (**A**) and (**B**) respectively. Columns and bars represent mean ± SD ($n = 3$ mice). Asterisks indicate significant differences compared with the WT group (*$p < 0.05$, ***$p < 0.001$, student's t tests). GSEA enrichment plots of representative gene sets that were significantly enriched in downregulated genes. Actin "cytoskeleton" (**E**) and "lysosome" (**F**) gene sets were downregulated in $CatB^{-/-}$ mouse hippocampus relative to that of WT mice. **G** CLSM images of Aβ (green), CD68 (red), and Iba1 (magenta) with Hoechst (blue) in the Aβ-injected area of WT and $CatB^{-/-}$ mouse hippocampus with microglia deletion. Scale bar, 50 μm. **H** Relative fluorescent density of Aβ in the images shown in (**G**). Columns and bars represent mean ± SD ($n = 4$ mice). Ns no significant difference (student's t test). **I–N** Hilyte Fluor-fAβ, and Hilyte Fluor-OAβ were incubated with MG6 and MG7 cells for the indicated time periods and analyzed by FACS (**I–L**) or confocal microscopy (**M, N**). Scale bar, 10 μm. Quantification of Hilyte Fluor-Aβ is shown in (**J, L**). Asterisks indicate significant differences compared with the MG6 group at the same time points (***$p < 0.001$, two-way ANOVA).

neurons with microglia or astrocytes in the Aβ injected area. A considerable number of neurons were located in the cell bodies of activated microglia, but they were rarely observed in astrocytes (Fig. 1E, F). These results indicate that Aβ increased CatB levels in microglia, which may modulate its Aβ clearance activity.

Next, we injected Aβ into the hippocampus of both WT and $CatB^{-/-}$ mice to examine the direct effects of CatB on Aβ clearance. Aβ immunolabeling suggested a marked reduction in Aβ clearance in $CatB^{-/-}$ mice relative to WT controls after Aβ administration for 1 and 3 weeks (Fig. 1G, H). Aβ remaining in the hippocampus was analyzed by ELISA, revealing significantly higher Aβ levels in $CatB^{-/-}$ than WT mice (Fig. 1I, J). In addition, relative to WT mice, $CatB^{-/-}$ mice showed significantly reduced numbers of movements and reduced time in the central area, but not total distance, after Aβ administration for 3 weeks (Fig. 1K–N). We also evaluated spatial learning and memory ability using the Y-maze test, and 3 weeks of Aβ administration led to significantly less spontaneous alterations in $CatB^{-/-}$ mice than in WT mice (Fig. 1O). These results suggest that CatB is involved in Aβ clearance, which is associated with spatial learning and memory in the acute Aβ injection mouse model.

CatB-induced transcriptional changes in the hippocampus after Aβ injection

We aimed to evaluate changes in gene expression induced by CatB. Hence, we undertook bulk RNA-seq analysis of WT and $CatB^{-/-}$ mice after treatment with Aβ or saline for 1 week. A total of 182 DEGs were detected in WT and $CatB^{-/-}$ mice hippocampal tissue after Aβ injection (Fig. S1A). Heatmaps and hierarchal clustering of hippocampus transcripts in different genetic groups are presented in Fig. S1B. Subsequently, we analyzed DEG function and potential shared signaling pathways using the Gene Ontology (GO) database and Database for Annotation, Visualization, and Integrated Discovery. GO covers three domains: biological process, cellular component (CC), and molecular function (MF). The results indicated that most DEGs were involved in "membrane", "integral component of membrane" in the CC domain, suggesting that they may have important roles in cell movement (Fig. S1C). MF analysis indicated that most DEGs were involved in "protein binding", which may contribute to various types of cell recognition and signal transduction (Fig. S1D).

Further, comparative RNA-seq analysis of WT and $CatB^{-/-}$ hippocampus after Aβ injection indicated that a group of genes related to cell activation, migration, phagocytosis, or inflammation was significantly downregulated in $CatB^{-/-}$ hippocampus compared to that of WT mice (Fig. S2A, B). The top DEGs were further validated by q-PCR (Fig. S2C–H). Taken together, our data indicate that CatB may regulate microglial functions including migration, phagocytosis, and neuroinflammation.

Microglial CatB is involved in Aβ phagocytosis

Accumulations of microglia and astrocytes have been observed surrounding Aβ plaques in the AD brain [18]. To characterize the major cells responsible for phagocytosing Aβ, we co-stained Aβ

with astrocytes, microglia, and neurons in both WT and $CatB^{-/-}$ mice after Aβ injection. Almost all of the remaining Aβ detected was in microglia, but not in astrocytes or neurons (Fig. S3A–C). Intriguingly, remaining Aβ levels were markedly higher in $CatB^{-/-}$ mice than those in the WT mice (Fig. S3A–C). To further confirm the role of microglia in Aβ phagocytosis, we co-stained CD68 with Aβ and Iba1 in the hippocampus of WT and $CatB^{-/-}$ mice after Aβ injection, as CD68 is a general marker of activated phagocytic microglia in the brain [19]. CD68 signal was undetectable in the hippocampus of WT and $CatB^{-/-}$ mice after saline injection (Fig. 2A, B). However, CD68 immunoreactivity was detectable and significantly lower in hippocampus from $CatB^{-/-}$ mice than in corresponding samples from WT mice after Aβ injection for 1 week (Fig. 2A, C). Moreover, no CD68 immunoreactivity was detected in the hippocampus of WT mice after Aβ administration for 3 weeks, while it remained visible in $CatB^{-/-}$ mice (Fig. 2B, D), suggesting that WT, but not $CatB^{-/-}$, microglia almost cleared Aβ. Further, GSEA enrichment plots of representative gene sets showed that the "regulation of actin cytoskeleton" and "lysosome" gene sets were downregulated in the hippocampus of $CatB^{-/-}$ mice relative to WT mice (Fig. 2E, F). To confirm the role of microglial CatB in Aβ clearance, we pharmacologically eliminated microglia in WT and $CatB^{-/-}$ mice by oral administration of the microglia-depleting reagent, PLX (Fig. S4A, B). No difference in the amount of Aβ remaining after injection was detected between WT and $CatB^{-/-}$ mice following microglia deletion (Fig. 2G, H). These data suggest a vital role for microglial CatB in Aβ phagocytosis.

To further confirm that CatB regulates Aβ phagocytosis by microglia, we knocked down CatB in MG6 cells, and named the resulting cell line MG7. The efficiency of knockdown was validated by immunoblotting (Fig. S5A, B). Then, we conducted in vitro microglia phagocytosis assays using MG6 and MG7 cells treated with fluorescence-labeled Aβ. FACS assay suggested that MG7 cells showed a significant reduction in phagocytosis of both fAβ and OAβ (Fig. 2I–L). These results were further validated by immunostaining of Aβ in MG6 and MG7 cells (Fig. 2M, N). Moreover, inhibition of CatB activity also reduced the Aβ phagocytosis activity of primary microglia (Fig. S6A). To determine whether CatB-regulated microglial phagocytosis is specific for Aβ, we further examined the phagocytic activity of microglia by treatment with zymosan particles in cell culture. Relatively few particles were detected within MG7 cells relative to MG6 cells (Fig. S6 B, C). Collectively, these data support that CatB is involved in microglial phagocytosis of Aβ.

CatB regulates microglial migration in the presence of Aβ

We found that a large number of activated microglia accumulated in the Aβ-injected area (Figs. 1G, Hand 2A); therefore, we sought to determine the origin of these cells. First, we examined the possibility that the activated microglia were proliferating cells by staining for Ki67, a proliferation marker routinely used in pathology analysis [20], and found no obvious differences in Ki67 expression in microglia from WT and $CatB^{-/-}$ mice after Aβ injection (Fig. S7). Next, we examined the role of CatB in microglial

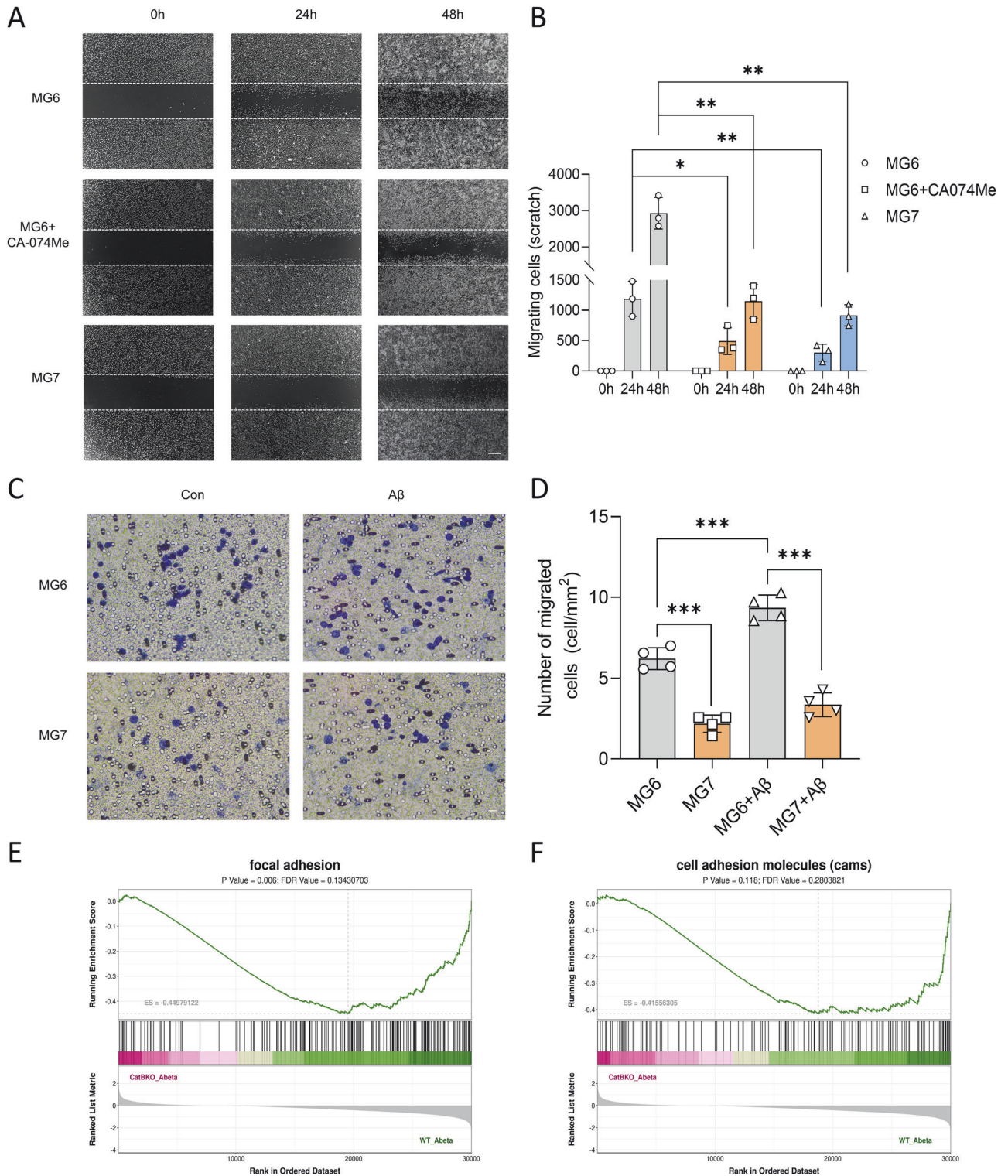**Fig. 3 CatB inhibition attenuates microglial migration. A** Bright-field images of MG6 and MG7 cells treated with or without CA-074Me at 0, 24, and 48 h after scratch damage. Scale bars, 100 μm. **B** Quantification of cell migration shown in (**A**). Columns and bars represent mean ± SD (*n* = three independent experiments). Asterisks indicate significant differences compared with the indicated group (*$p < 0.05$, **$p < 0.01$, one-way ANOVA). **C** Representative images of migrated MG6 and MG7 cells treated with or without Aβ. Microglial cells that migrated through a membrane were stained and counted. Scale bar, 10 μm. **D** Quantitative analysis of the number of migrated cells. Columns and bars represent mean ± SD (*n* = 4 independent experiments). Asterisks indicate significant differences compared with the indicated group (***$p < 0.001$, one-way ANOVA). **E**, **F** GSEA plots of representative gene sets significantly enriched for downregulated genes. The "focal adhesion" (**E**) and "cell adhesion molecules" (**F**) gene sets were downregulated in $CatB^{-/-}$ mouse hippocampus relative to that from wild-type (WT) mice.

migration in the presence of Aβ. In vitro cell scratch assay indicated that MG6 cells gradually migrated into the scratch; however, pharmacological or genetic inhibition of CatB significantly reduced microglial cell migration (Fig. 3A, B). In addition, in Boyden chamber assays, MG7 cells showed significantly less migration through polycarbonate membrane than MG6 cells after Aβ treatment for 48 h (Fig. 3C, D). Moreover, GSEA indicated that the "focal adhesion" (Fig. 3E) and "cell adhesion molecules" (Fig. 3F) gene sets were downregulated in $CatB^{-/-}$ mouse hippocampus relative to that of WT mice (Fig. 3E, F). These results

suggest the involvement of CatB in microglial migration in the presence of Aβ.

CatB regulates microglia-mediated neuroinflammation after Aβ treatment

In AD, Aβ has been shown to activate microglia, which induces neuroinflammation by releasing inflammatory cytokines. Therefore, we investigated whether CatB can influence microglia inflammatory responses stimulated by Aβ. MG6 and MG7 cells were treated with Aβ for 24 h, followed by analysis of $CatB$, $IL-1\beta$,
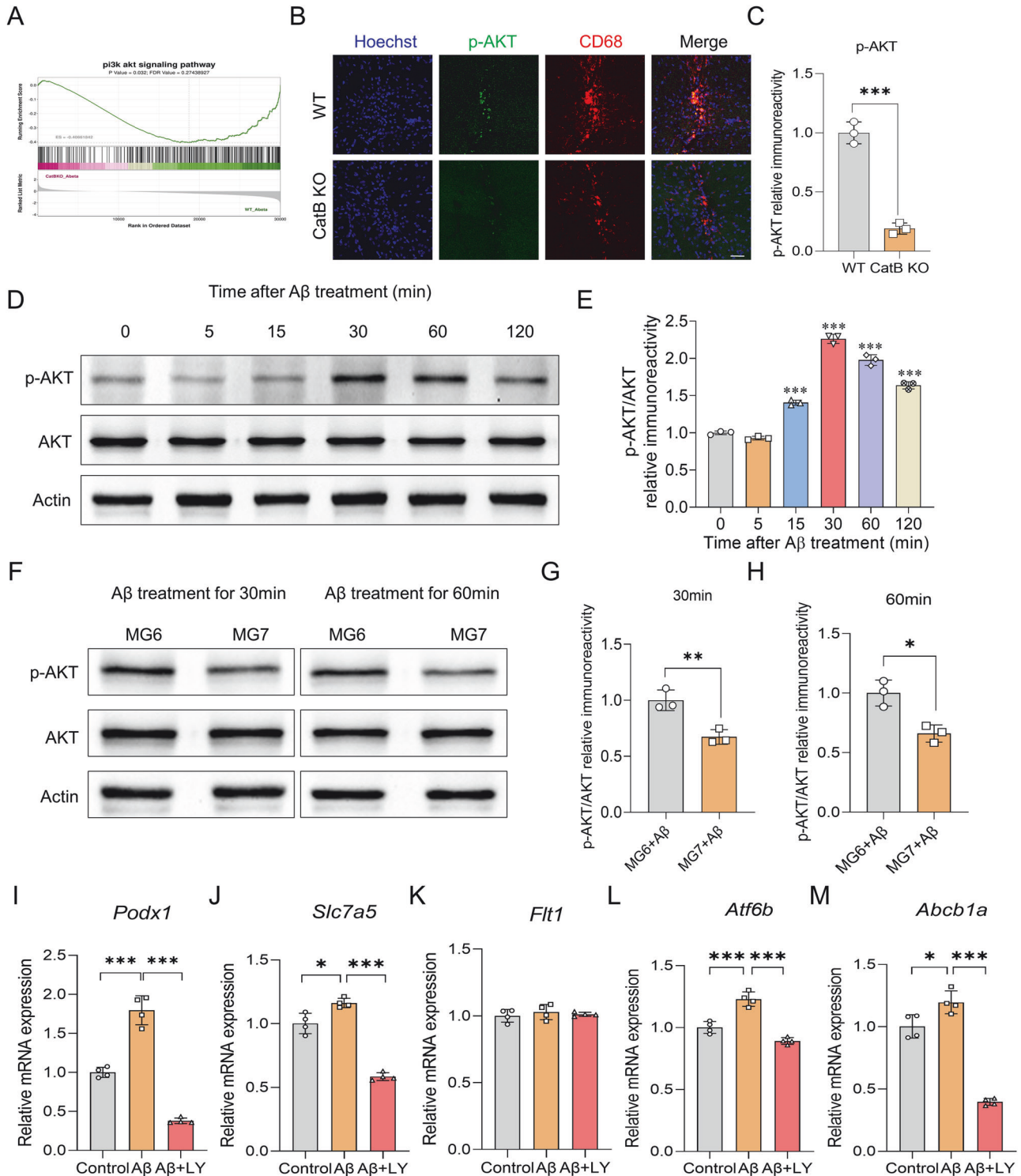
Fig. 4   CatB is involved in the PI3K-Akt pathway in microglia treated with Aβ. A GSEA plots of representative gene sets demonstrating that the "PI3K-AKT signaling pathway" was downregulated in hippocampus from $CatB^{-/-}$ mice compared to that of wild-type (WT) mice. **B** Confocal laser scanning microscope images of p-AKT (green), CD68 (red), and Hoechst (blue) in the injected area of the hippocampus of WT mice and $CatB^{-/-}$ mice after Aβ administration for 1 week. Scale bar, 50 μm. **C** Relative fluorescent density of p-Akt in the images shown in (**B**). Columns and bars represent mean ± SD ($n = 3$ mice). Asterisks indicate significant differences compared with the WT group (***$p < 0.001$, Student's t tests). **D** Immunoblots of p-AKT and AKT in MG6 cells treated with Aβ at 0, 5, 15, 30, 60, and 120 min. **E** Quantitative analysis of p-AKT/AKT shown in (**D**). Columns and bars represent mean ± SD ($n = 3$ independent experiments). Asterisks indicate significant differences compared with the control group (***$p < 0.001$, one-way ANOVA). **F** Immunoblots of p-AKT and AKT in MG6 and MG7 cells treated with Aβ for 30 or 60 min. Quantitative analysis of p-AKT/AKT in MG6 and MG7 cells treated with Aβ for 30 (**G**) or 60 (**H**) min. Columns and bars represent the mean ± SD ($n = 3$ independent experiments). Asterisks indicate significant differences compared with the indicated group (*$p < 0.05$, **$p < 0.01$, one-way ANOVA). Relative mRNA expression of Podx1 (**I**), Slc7a5 (**J**), Flt1 (**K**), Atf6b (**L**), and Abcb1a (**M**) in MG6 cells treated with Aβ for 24 h. LY, a synthetic PI3K inhibitor was pretreated. Columns and bars represent the mean ± SD ($n = 4$ independent experiments). Asterisks indicate significant differences compared with the indicated group (*$p < 0.05$, ***$p < 0.001$, one-way ANOVA).

TNF-α, and *NOS2* mRNA levels. The mRNA expression levels of these inflammatory mediators were significantly increased in MG6, but not MG7 cells (Fig. S8A–D). The protein amount of IL-1β and TNFα were also significantly increase in MG6 cells, but not MG7 cells after treatment with Aβ for 24 h (Fig. S8E, F). Furthermore, in vivo experiments showed reduced activation of microglia or astrocytes, evidenced by changes in Iba1 and GFAP protein levels, in $CatB^{-/-}$ mouse hippocampus relative to levels in WT mice at 1 week, but not at 3 weeks, after Aβ treatment (Fig. S8G–L). Collectively, our data suggest a crucial regulatory role for CatB in microglia-mediated acute neuroinflammation after Aβ treatment.

CatB activates the PI3K-Akt signaling pathway in microglia after Aβ treatment

Emerging evidence suggests that the PI3K-Akt pathway plays a critical role in modulating microglial function [21]. Consistently, our GSEA plots indicated that "PI3K-Akt signal pathway" gene sets were downregulated in $CatB^{-/-}$ mouse hippocampus relative to levels in WT mice at 1 week after Aβ treatment (Fig. 4A). Immunofluorescent signals of p-Akt showed colocalization with CD68$^+$ microglia and a significant reduction in the Aβ-injected area of $CatB^{-/-}$ mice compared to WT mice (Fig. 4B, C). We further investigated whether CatB exerts its modulation of microglial function through the PI3K-Akt signaling pathway. As shown in Fig. 4D, E, PI3K-Akt signaling was significantly activated and peaked at 30 min following Aβ treatment. Moreover, levels of p-AKT/AKT were significantly lower in MG7 cells than those in MG6 cells at 30 and 60 min after Aβ treatment (Fig. 4F–H). These results demonstrate that CatB regulates activation of the PI3K-Akt signaling pathway in microglia on Aβ treatment. To investigate the regulatory effects of PI3K-Akt signaling on microglial function, we used the PI3K/Akt inhibitor, LY294002 (2 μM), to block PI3K-Akt pathway activation in MG6 cells (Fig. S9). Inhibition of PI3K/Akt significantly attenuated the Aβ-induced increase in the expression of genes modulating microglial migration, phagocytosis, and acute neuroinflammation, including *Podx1*, *Slc7a5*, *Atf6b*, and *Abcb1a* (Fig. 4I–M). Together, these data suggest that CatB modulates microglial function through activation of the PI3K-Akt signaling pathway.

Insufficient Aβ clearance by MG7 cells mediated neuronal toxicity

Given the differential Aβ clearance capacity of MG6 and MG7 cells, we next examined the effects of Aβ-treated MG6 and MG7 cells on neurons. Visible Aβ signals were detected within the cells at 0.5, 2, 6, and 12 h after Aβ treatment, while no signals were visible at 0 or 24 h (Fig. 5A), consistent with a previous report [22]. In MG6 cells, Aβ signals peaked at 2 h and gradually decreased until 24 h after Aβ treatment, suggesting the processes of Aβ phagocytosis mainly occurred within 2 h, and degradation by microglia mainly occurred after 2 h (Fig. 5A). Therefore, we collected microglial conditioned medium (MCM) from MG6 and MG7 cells 2 h after Aβ treatment and then applied the MCM in WT primary neuron cultures (Fig. 5B). Expression levels of postsynaptic density 95

(PSD95) and synaptophysin (SYN) strongly correspond with synapse numbers [23]; thus, PSD95 and SYN protein expression was measured by immunolabeling to evaluate neuronal activity. At 24 h after incubation with MCM from Aβ-treated MG6 or MG7, primary neurons showed significant reductions in both SYN and PSD95 levels (Fig. 5C–E). These results suggest that insufficient clearance of Aβ by microglia induces neuronal toxicity.

DISCUSSION

How microglia modulate the Aβ burden during AD is not fully understood. As failure to clear Aβ is assumed to contribute to sporadic AD, it is of great relevance to gain more insights into the clearance mechanisms involved. In this study, we used an acute intracerebral Aβ injection mouse model to observe the regulation of microglial clearance of Aβ in the absence of any new Aβ production. Our data suggest two main findings: first, CatB is crucial for Aβ clearance by microglia; and second, CatB modulates microglial migration, neuroinflammation, and phagocytosis through activation of PI3K-Akt signaling (Fig. S10).

The role of CatB in cognitive function remains controversial. CatB overexpression in hippocampal neurons using adeno-associated virus serotype 2/1 is reported to ameliorate AD-like pathologies, including Aβ production in the mouse brain and impairments in learning and memory [11]; however, pharmacological or genetic inhibition of CatB decreases Aβ levels and improves memory function in mouse models of AD [24–26]. Further, CatB is reported to have beneficial effects on cognition, including enhancing hippocampal neurogenesis and spatial memory in mice following exercise [27]. We previously reported that CatB is expressed in both microglia and neurons in aged mouse brains [17]; hence, differential roles of CatB in microglia and neurons could be a possible explanation for the discrepant finding regarding the role of CatB in cognitive function. In AD, Aβ accumulation in the brain arises from an imbalance of Aβ production and clearance; however, Aβ production and clearance occur simultaneously in AD transgenic mice, which makes precise study of pure clearance pathways challenging. Therefore, to avoid the effects of CatB in Aβ production by neurons in the hippocampus of brain, we stereotaxically injected Aβ into the hippocampus of WT and $CatB^{-/-}$ mice, allowing examination of the specific role of CatB in Aβ clearance. We found that CatB deficiency led to relatively poor Aβ clearance accompanied by worsened cognitive impairment. Therefore, our data demonstrate that CatB plays a vital role in microglial clearance of Aβ, at least in young microglia. Similar results have also been reported in HL60 cells, a human acute promyelocytic cell line. CatB inhibitor significantly inhibited the phagocytic activity of HL60 cells in the presence of wheat bran arabinoxylan [28]. Hence, it could conceivably be hypothesized that CatB may regulate phagocytosis in phagocytes, not limited to microglia.

Evidence supporting a decline in microglial phagocytosis during aging comes from studies focusing on the ability of isolated
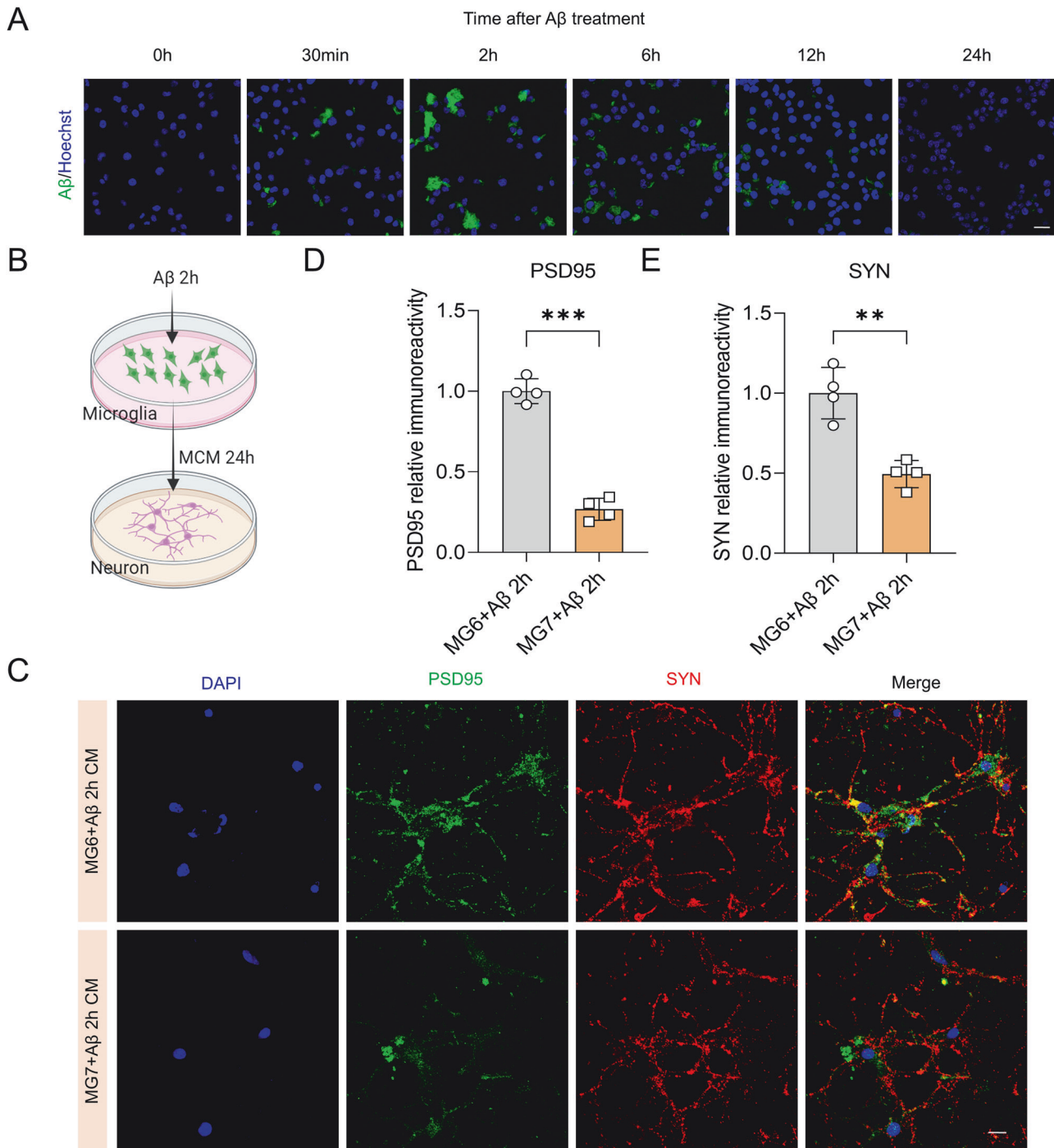
Fig. 5 CatB-deficient microglia mediate toxic effects on neurons through insufficient Aβ clearance. A CLSM images of Aβ (green) and Hoechst (blue) in MG6 cells after treatment with Aβ for 0, 0.5, 2, 6, 12, and 24 h. Scale bar, 30 μm. **B** Schematic illustration of neuron cultures in microglial conditioned medium (MCM) from MG6 or MG7 cells after Aβ treatment for 2 h. **C** CLSM images of PSD95 (green), SYN (red), and Hoechst (blue) in primary neurons treated with MCM from MG6 and MG7 cells prepared as for (**B**). Scale bar, 20 μm. Analysis of PSD95 (**D**) and SYN (**E**) puncta in (**C**). Columns and bars represent mean ± SD ($n = 4$ independent experiments). Asterisks indicate significant differences compared with the control group (**$p < 0.01$, ***$p < 0.001$, Student's t test).

microglia from young and aged mice to internalize and degrade monomeric, oligomeric, and fibrillary Aβ. Compared with microglia from young mice, those from aged mice internalize less Aβ and, consequently, degrade it to a lesser extent [29, 30]. Our experiments were confined to observation of the regulatory role of CatB in young microglia. It will be interesting to examine the expression and enzymatic activity of CatB, and its modulatory function, in aged microglia, since aged microglial phagocytotic activity can be reversible to limit amyloid accumulation [31]. Recently, there has been great progress in clinical trials of AD treatment with anti-Aβ monoclonal antibodies. A crucial feature shared by these monoclonal antibodies is their ability to engage soluble Aβ, albeit to various degrees, resulting in reinforced phagocytic clearance. Lecanemab has been approved by the FDA for treatment of patients with early, but not late, AD; however, the clinical effects of these agents are modest and associated with

amyloid-related imaging abnormalities. Ongoing and future research is focused on identification of more potent and safer agents.

The PI3K-Akt cascade is a highly conserved intracellular signaling pathway present in all eukaryotic cells, that acts as a central node for transduction of extracellular stimuli, and is recognized as the central regulator of microglial activity in response to extrinsic stimuli [32]. Consistently, our in vivo and in vitro data suggest that PI3K-Akt signaling is critical for microglial function modulation in response to Aβ; however, CatB deficiency significantly inhibited Aβ-induced activation of PI3K-Akt signaling. Although we did not further dissect how CatB activates PI3K-Akt signaling in microglia on Aβ treatment, it has been reported that CatB-mediated PI3K-Akt activation is dependent on integrin αvβ3, also known as the vitronectin receptor [33]; however, the relationship between CatB and integrin αvβ3 requires further confirmation. Interestingly, PI3K-Akt activation is unaltered in a neuronal cell line (N2a) after CatB inhibition [34], suggesting different roles for CatB in microglia and neurons.

Key unresolved questions include whether microglial dysfunction in AD is reversible and whether microglial phagocytic ability can be restored to limit amyloid accumulation. In an ex vivo model of amyloid plaque clearance by co-culture of young WT brain slices together with brain slices from aged AD mice, functional impairment of aged microglial cells in amyloid plaque-bearing tissue could be reversed by factors secreted from young microglia, suggesting that young microglia can restore amyloid plaque clearance by aged microglia [31]. To explore whether replacement of aged microglia with new cells affects and shapes the resultant tissue, a CSF1R inhibitor was used to induce microglial elimination and repopulation, which demonstrated that broad reversals in many age-related changes in the brain can be achieved through microglial repopulation [35]. Our results indicate that CatB is critical to regulation of microglial clearance of Aβ, suggesting that CatB may also have an important role in aging; however, CatB was found to increase in aged microglia and translocate to the cytosol or nucleus, resulting in microglia-mediated chronic neuroinflammation [17, 36, 37]. These results suggest that the role of CatB alters with aging, and these functional changes may be due to changes in CatB-extra-lysosomal distribution or optimal CatB substrates.

Microglial phagocytosis is believed to gradually become compromised during AD progression, and this impairment correlates with increased production of proinflammatory cytokines and overwhelming accumulation of Aβ plaques in the AD brain. To investigate the relationship between inflammation and Aβ phagocytosis, Babcock et al. examined the phagocytic index and total Aβ load in cytokine-producing and non-cytokine-producing subsets of $CD11b^+CD45^+$ microglia from the neocortex of 21-month-old APP/PS1 transgenic mice [38]. The authors found that phagocytic index was unrelated to IL-1β levels, consistent with another study showing no effect of adenoviral overexpression of IL-1β on either the percentage of methoxy-XO4+ (MXO4+) microglia, representing cells containing amyloid plaques, or the amount of fAβ internalized by individual microglia. Instead, the observed reduction in Aβ plaques could be attributed to an increase in the total number of MXO4+ microglia, as consequence of IL-1β-induced microglial proliferation [39]. In response to exogenous Aβ, $CatB^{-/-}$ mice microglia exhibited compromised phagocytosis and mice had lower levels of neuroinflammation, accompanied by impaired cognitive function, relative to WT mice. Moreover, the injected Aβ remained in the hippocampus of $CatB^{-/-}$ mice after Aβ injection for 3 weeks; therefore, it is reasonable to hypothesize that the relatively poor cognitive function of $CatB^{-/-}$ mice was due to residual Aβ in the hippocampus.

In the present study, we used MG6 cells to study molecular events associated with Aβ phagocytosis, migration and inflammatory responses. While the cell model has been used for shaping our current knowledge of AD pathology, the chromic nature of neurodegeneration should be complemented by human tissue. Further study using AD patient induced pluripotent stem cell (ipsc)-derived microglia will strengthen our findings. We demonstrated the regulatory role of CatB in PI3K-Akt pathway in microglia in the presence of Aβ, however, we haven't analyzed the upstream receptors and the specific targets of CatB in regulating this pathway. Moreover, the absence of behavioral tests for saline-injected controls and the absence of single-cell RNA sequencing in microglia are also key limitations in this study.

CONCLUSION
In summary, our findings illustrate that inhibition of CatB impaired the clearance of Aβ by microglia in the brain, which is related to cognitive decline in mice. Our data supported a critical role of CatB in modulating microglial function including migration, phagocytosis, and inflammatory responses up on Aβ, which is depending on PI3K-Akt signaling pathway. These findings have valuable implications for the development of novel therapeutic approaches to remodel microglial functions in Aβ-associated diseases.

DATA AVAILABILITY
All data supporting the conclusions of this article are included within the article and the additional files.

REFERENCES
1. Jack CR Jr, Bennett DA, Blennow K, Carrillo MC, Dunn B, Haeberlein SB, et al. NIA-AA research framework: toward a biological definition of Alzheimer's disease. Alzheimers Dement. 2018;14:535–62.
2. van Dyck CH, Swanson CJ, Aisen P, Bateman RJ, Chen C, Gee M, et al. Lecanemab in early Alzheimer's disease. N Engl J Med. 2023;388:9–21.
3. Ni J, Wu Z, Peterts C, Yamamoto K, Qing H, Nakanishi H. The critical role of proteolytic relay through cathepsins B and E in the phenotypic change of microglia/macrophage. J Neurosci. 2015;35:12488–501.
4. Butler CA, Popescu AS, Kitchener EJA, Allendorf DH, Puigdellivol M, Brown GC. Microglial phagocytosis of neurons in neurodegeneration, and its regulation. J Neurochem. 2021;158:621–39.
5. Keren-Shaul H, Spinrad A, Weiner A, Matcovitch-Natan O, Dvir-Szternfeld R, Ulland TK, et al. A unique microglia type associated with restricting development of Alzheimer's disease. Cell. 2017;169:1276–90.e17.
6. Deczkowska A, Keren-Shaul H, Weiner A, Colonna M, Schwartz M, Amit I. Disease-associated microglia: a universal immune sensor of neurodegeneration. Cell. 2018;173:1073–81.
7. Barrett AJ. Human cathepsin B1. purification and some properties of the enzyme. Biochem J. 1973;131:809–22.
8. Xie Z, Zhao M, Yan C, Kong W, Lan F, Narengaowa, et al. Cathepsin B in programmed cell death machinery: mechanisms of execution and regulatory pathways. Cell Death Dis. 2023;14:255.
9. Wu Z, Ni J, Liu Y, Teeling JL, Takayama F, Collcutt A, et al. Cathepsin B plays a critical role in inducing Alzheimer's disease-like phenotypes following chronic systemic exposure to lipopolysaccharide from Porphyromonas gingivalis in mice. Brain Behav Immun. 2017;65:350–61.
10. Sun B, Zhou Y, Halabisky B, Lo I, Cho SH, Mueller-Steiner S, et al. Cystatin C-cathepsin B axis regulates amyloid beta levels and associated neuronal deficits in an animal model of Alzheimer's disease. Neuron. 2008;60:247–57.
11. Embury CM, Dyavarshetty B, Lu Y, Wiederin JL, Ciborowski P, Gendelman HE, et al. Cathepsin B improves ss-amyloidosis and learning and memory in models of Alzheimer's disease. J Neuroimmune Pharmacol. 2017;12:340–52.
12. Liu Y, Wu Z, Zhang X, Ni J, Yu W, Zhou Y, et al. Leptomeningeal cells transduce peripheral macrophages inflammatory signal to microglia in reponse to Porphyromonas gingivalis LPS. Mediators Inflamm. 2013;2013:407562.
13. Ni J, Wu Z, Meng J, Saito T, Saido TC, Qing H, et al. An impaired intrinsic microglial clock system induces neuroinflammatory alterations in the early stage of amyloid precursor protein knock-in mouse brain. J Neuroinflammation. 2019;16:173.
14. Czirr E, Castello NA, Mosher KI, Castellano JM, Hinkson IV, Lucin KM, et al. Microglial complement receptor 3 regulates brain Aβ levels through secreted proteolytic activity. J Exp Med. 2017;214:1081–92.

15. Xie Z, Meng J, Wu Z, Nakanishi H, Hayashi Y, Kong W, et al. The dual nature of microglia in Alzheimer's disease: a microglia-neuron crosstalk perspective. Neuroscientist. 2022;29:616–38.

16. Stoka V, Turk V, Turk B. Lysosomal cathepsins and their regulation in aging and neurodegeneration. Ageing Res Rev. 2016;32:22–37.

17. Ni J, Wu Z, Stoka V, Meng J, Hayashi Y, Peters C, et al. Increased expression and altered subcellular distribution of cathepsin B in microglia induce cognitive impairment through oxidative stress and inflammatory response in mice. Aging Cell. 2019;18:e12856.

18. Saito T, Matsuba Y, Mihira N, Takano J, Nilsson P, Itohara S, et al. Single App knock-in mouse models of Alzheimer's disease. Nat Neurosci. 2014;17:661–3.

19. Perego C, Fumagalli S, De Simoni MG. Temporal pattern of expression and colocalization of microglia/macrophage phenotype markers following brain ischemic injury in mice. J Neuroinflammation. 2011;8:174.

20. Uxa S, Castillo-Binder P, Kohler R, Stangner K, Muller GA, Engeland K. Ki-67 gene expression. Cell Death Differ. 2021;28:3357–70.

21. Chu E, Mychasiuk R, Hibbs ML, Semple BD. Dysregulated phosphoinositide 3-kinase signaling in microglia: shaping chronic neuroinflammation. J Neuroinflammation. 2021;18:276.

22. Zhao Y, Wu X, Li X, Jiang L-L, Gui X, Liu Y, et al. TREM2 is a receptor for β-amyloid that mediates microglial function. Neuron. 2018;97:1023–31.

23. Matosin N, Fernandez-Enright F, Lum JS, Engel M, Andrews JL, Gassen NC, et al. Molecular evidence of synaptic pathology in the CA1 region in schizophrenia. NPJ Schizophr. 2016;2:16022.

24. Hook VY, Kindy M, Hook G. Inhibitors of cathepsin B improve memory and reduce beta-amyloid in transgenic Alzheimer disease mice expressing the wild-type, but not the Swedish mutant, beta-secretase site of the amyloid precursor protein. J Biol Chem. 2008;283:7745–53.

25. Kindy MS, Yu J, Zhu H, El-Amouri SS, Hook V, Hook GR. Deletion of the cathepsin B gene improves memory deficits in a transgenic ALZHeimer's disease mouse model expressing AbetaPP containing the wild-type beta-secretase site sequence. J Alzheimers Dis. 2012;29:827–40.

26. Hook VY, Kindy M, Reinheckel T, Peters C, Hook G. Genetic cathepsin B deficiency reduces beta-amyloid in transgenic mice expressing human wild-type amyloid precursor protein. Biochem Biophys Res Commun. 2009;386:284–8.

27. Moon HY, Becke A, Berron D, Becker B, Sah N, Benoni G, et al. Running-induced systemic cathepsin B secretion is associated with memory function. Cell Metab. 2016;24:332–40.

28. Monobe M, Katayanagi Y, Maeda-Yamamoto M, Hiramoto S. Enhancement of the immunostimulatory activity of 1,25-dihydroxyvitamin D3-differentiated HL60 cells with an arabinoxylan from wheat bran. Food Sci Technol Res. 2012;18:481–84.

29. Njie EG, Boelen E, Stassen FR, Steinbusch HW, Borchelt DR, Streit WJ. Ex vivo cultures of microglia from young and aged rodent brain reveal age-related changes in microglial function. Neurobiol Aging. 2012;33:195.e1–12.

30. Floden AM, Combs CK. Microglia demonstrate age-dependent interaction with amyloid-beta fibrils. J Alzheimers Dis. 2011;25:279–93.

31. Daria A, Colombo A, Llovera G, Hampel H, Willem M, Liesz A, et al. Young microglia restore amyloid plaque clearance of aged microglia. EMBO J. 2017;36:583–603.

32. Tarassishin L, Suh HS, Lee SC. Interferon regulatory factor 3 plays an anti-inflammatory role in microglia by activating the PI3K/Akt pathway. J Neuroinflammation. 2011;8:187.

33. Xu ZZ, Xiu P, Lv JW, Wang FH, Dong XF, Liu F, et al. Integrin alphavbeta3 is required for cathepsin B-induced hepatocellular carcinoma progression. Mol Med Rep. 2015;11:3499–504.

34. Jiang M, Meng J, Zeng F, Qing H, Hook G, Hook V, et al. Cathepsin B inhibition blocks neurite outgrowth in cultured neurons by regulating lysosomal trafficking and remodeling. J Neurochem. 2020;155:300–12.

35. Elmore MRP, Hohsfield LA, Kramár EA, Soreq L, Lee RJ, Pham ST, et al. Replacement of microglia in the aged brain reverses cognitive, synaptic, and neuronal deficits in mice. Aging Cell. 2018;17:e12832.

36. Meng J, Liu Y, Xie Z, Qing H, Lei P, Ni J. Nucleus distribution of cathepsin B in senescent microglia promotes brain aging through degradation of sirtuins. Neurobiol Aging. 2020;96:255–66.

37. Ni J, Lan F, Xu Y, Nakanishi H, Li X. Extralysosomal cathepsin B in central nervous system: mechanisms and therapeutic implications. Brain Pathol. 2022;32:e13071.

38. Babcock AA, Ilkjaer L, Clausen BH, Villadsen B, Dissing-Olesen L, Bendixen AT, et al. Cytokine-producing microglia have an altered beta-amyloid load in aged APP/PS1 Tg mice. Brain Behav Immun. 2015;48:86–101.

39. Rivera-Escalera F, Pinney JJ, Owlett L, Ahmed H, Thakar J, Olschowka JA, et al. IL-1beta-driven amyloid plaque clearance is associated with an expansion of transcriptionally reprogrammed microglia. J Neuroinflammation. 2019;16:261.

AUTHOR CONTRIBUTIONS

JN designed the research and wrote the manuscript; MJ performed most of the experiments and data analysis and wrote the manuscript. DZ, YZ, WK, and ZX performed part of the animal experiments. YX and YL conducted cell culture. SZ, XK, SZ, and RM analyzed data. YP, ZW, HN, JZ, HL, and ZQ provided the reagents. LL and HQ provided helpful suggestions to the manuscript. All the authors read and approved the final manuscript.

COMPETING INTERESTS
The author declares no competing interests.

ETHICS APPROVAL
All animal care and experimental procedures were approved by the Institutional Animal Care and Use Committee of the Beijing Institute of Technology (BIT-EC-SCXK2018-0003-M-2021028) in conformity with the international guidelines on the ethics of animal experimentation.

ADDITIONAL INFORMATION
Supplementary information The online version contains supplementary material available at https://doi.org/10.1038/s41386-024-01994-0.

Correspondence and requests for materials should be addressed to Li Lin or Junjun Ni.

Reprints and permission information is available at http://www.nature.com/reprints

Publisher's note Springer Nature remains neutral with regard to jurisdictional claims in published maps and institutional affiliations.